Critical role for bone marrow stromal antigen 2 in acute Chikungunya virus infection

Wadie D. Mahauad-Fernandez,[1,2] Philip H. Jones[1] and Chioma M. Okeoma[1,2]

[1]Department of Microbiology, Carver College of Medicine, University of Iowa, Iowa City, IA, USA

[2]Interdisciplinary Graduate Program in Molecular and Cellular Biology (MCB), University of Iowa, Iowa City, IA, USA

Correspondence
Chioma M. Okeoma
chioma-okeoma@uiowa.edu

Received 4 June 2014
Accepted 16 July 2014

Bone marrow stromal antigen 2 (BST-2; also known as tetherin or CD317) is an IFN-inducible gene that functions to block the release of a range of nascent enveloped virions from infected host cells. However, the role of BST-2 in viral pathogenesis remains poorly understood. BST-2 plays a multifaceted role in innate immunity, as it hinders retroviral infection and possibly promotes infection with some rhabdo- and orthomyxoviruses. This paradoxical role has probably hindered exploration of BST-2 antiviral function *in vivo*. We reported previously that BST-2 tethers Chikungunya virus (CHIKV)-like particles on the cell plasma membrane. To explore the role of BST-2 in CHIKV replication and host protection, we utilized CHIKV strain 181/25 to examine early events during CHIKV infection in a BST-2$^{-/-}$ mouse model. We observed an interesting dichotomy between WT and BST-2$^{-/-}$ mice. BST-2 deficiency increased inoculation site viral load, culminating in higher systemic viraemia and increased lymphoid tissues tropism. A suppressed inflammatory innate response demonstrated by impaired expression of IFN-α, IFN-γ and CD40 ligand was observed in BST-2$^{-/-}$ mice compared with the WT controls. These findings suggested that, in part, BST-2 protects lymphoid tissues from CHIKV infection and regulates CHIKV-induced inflammatory response by the host.

INTRODUCTION

Infection with the alphavirus Chikungunya virus (CHIKV) causes disease in a wide range of animals and humans following infected mosquitoes bites (Pialoux *et al.*, 2007). Clinical manifestations of infection include fever, skin rash, myalgia, and polyarthralgia accompanied by swollen ankles, knees and wrists (Powers & Logue, 2007). Although the mechanisms for viral pathogenesis and host protection are poorly understood, the host immune/inflammatory responses are thought to mediate viral clearance and, in most cases, initiate subsequent CHIKV-induced arthralgia/arthritic sequelae. Many human and murine cells are susceptible to CHIKV infection, and may play a role in CHIKV-induced pathology (Labadie *et al.*, 2010). Among these are myeloid and lymphoid cells, fibroblasts, and epithelial cells (Das *et al.*, 2010; Her *et al.*, 2010; Labadie *et al.*, 2010; Sourisseau *et al.*, 2007; Wikan *et al.*, 2012). The susceptibility of various host cells/tissues to CHIKV is beginning to unravel; however, the factors that regulate CHIKV tropism are poorly understood.

Host innate cellular factors have been shown to predict response to CHIKV (Olagnier *et al.*, 2014; Partidos *et al.*, 2011; Schilte *et al.*, 2010; Seymour *et al.*, 2013; Wauquier *et al.*, 2011; Werneke *et al.*, 2011). Signalling through type 1 IFN receptor (IFN-α/βR) plays a role in controlling CHIKV infection and CHIKV-induced arthritogenic disease (Briolant *et al.*, 2004; Couderc *et al.*, 2008, 2009; Gardner *et al.*, 2012; Partidos *et al.*, 2011; Schilte *et al.*, 2010). Nonetheless, IFN-α/βR-independent control of CHIKV has been reported (Olagnier *et al.*, 2014; Partidos *et al.*, 2011). Our previous studies revealed that the host restriction factor (HRF) called bone marrow stromal antigen 2 (BST-2; also known as tetherin or CD317) retains budding CHIKV virus-like particles on the cell membrane and that CHIKV non-structural protein 1 (nsP1) counteracted BST-2-mediated tethering of CHIKV (Jones *et al.*, 2013b), signifying that BST-2 may be an essential HRF against CHIKV.

BST-2 is an IFN-inducible factor that tethers various nascent enveloped viruses on the cell surface (Douglas *et al.*, 2010; Jones *et al.*, 2012, 2013b; Lopez *et al.*, 2012; Neil *et al.*, 2008; Radoshitzky *et al.*, 2010). In addition to tethering, BST-2 plays a multifaceted role in innate immunity by possibly promoting infection with vesicular stomatitis virus, a rhabdovirus (Swiecki *et al.*, 2012), orthomyxoviruses such as influenza B virus (Swiecki *et al.*, 2012), and inhibiting replication of retroviruses as in human

One supplementary figure is available with the online version of this paper.

immunodeficiency virus type 1 (HIV-1) (Neil *et al.*, 2008), mouse mammary tumor virus (Jones *et al.*, 2012) and murine leukemia virus (Liberatore & Bieniasz, 2011). BST-2 may mediate its antiviral effect by modulating the induction of pro-inflammatory gene expression through NFκB (Galão *et al.*, 2012; Tokarev *et al.*, 2013) and inducing antibody-dependent cell cytotoxicity (Arias *et al.*, 2014; Pham *et al.*, 2014). These multifaceted and probably contradictory roles have hindered exploration of BST-2 antiviral function *in vivo*.

In the present study, we undertook experiments to probe the role of BST-2 in acute CHIKV replication and host protection. We utilized the live-attenuated CHIKV 181/25 strain developed at the US Army Medical Research Institute of Infectious Diseases (Levitt *et al.*, 1986) that produces non-lethal infection in WT mice (Gardner *et al.*, 2012) and can be safely used under biosafety level 2 conditions. This model allows evaluation of CHIKV-mediated alteration of host response in immunocompromised mice. As early events are more likely to be causal than events that are observed after the onset of disease symptoms and sequelae, our studies were conducted 24 h post-infection. We found that BST-2 deficiency was associated with high systemic viraemia, increased virus spread to distant tissues, enhanced lymphoid tissues tropism, and suppressed expression of IFN-α, IFN-γ and CD40 ligand (CD40L).

RESULTS

BST-2 restricts release of CHIKV 181/25 from both human and murine cells

We reported previously that BST-2 retains CHIKV virus-like particles on the cell surface (Jones *et al.*, 2013b). To determine whether BST-2 had any effect on the release of infectious virions, we performed virus release assays in different human cells infected with CHIKV 181/25 (m.o.i. 0.1). HeLa cells expressing high BST-2 produced significantly less virus compared with 293T cells expressing less BST-2 as determined by end-point dilution assay (EPDA) (Figs 1a–c and S1, available in the online Supplementary Material). Treatment of HeLa cells with IFN-α had no effect on BST-2 expression (Fig. 1a), but IFN-α increased BST-2 expression in 293T cells (Fig. 1b). The absence of an IFN-α effect on BST-2 induction in HeLa cells correlated with no change in virus release, whilst the increase in BST-2 expression in 293T cells correlated with a decrease in the amount of virions released into the extracellular milieu (Fig. 1c). These results suggested that induction of BST-2 with IFN-α had the potential to block CHIKV release from epithelial-like 293T cells.

To evaluate if IFN-α-induced BST-2 would have any effect on myeloid-like cells, human monocytic U937 cells were treated with PBS or IFN-α followed by infection with CHIKV. U937 cells, like other myeloid and lymphoid cells, express BST-2 (Fig. S1) and treatment with IFN-α enhanced BST-2 expression (Fig. 1d). Upon infection with CHIKV, U937 cells treated with IFN-α released fewer virions into the culture medium compared with cells treated with PBS (Fig. 1e). These data suggested that endogenous BST-2 induced by IFN-α may play a role in inhibiting CHIKV release from infected U937 cells. It appeared that the steady level of BST-2 in HeLa, 293T and U937 cells may have contributed to their ability to respond to CHIKV infection.

Next, we pre-treated immortalized WT and BST-2$^{-/-}$ mouse embryonic fibroblasts (MEFs) with PBS or IFN-β prior to infection, and showed that IFN-β induced BST-2 expression in immortalized WT MEFs, but not in BST-2$^{-/-}$ MEFs (Fig. 1f). The induction of BST-2 in WT MEFs resulted in inhibition of virus release (Fig. 1g) as determined by EPDA. As EPDA only measured infectious virus, we sought to determine the total viral titre (number of infectious and non-infectious viruses) produced by each genotype. For this purpose, we employed the nanoparticle tracking analysis (NTA) method. Using the NTA system (Du *et al.*, 2010; Filipe *et al.*, 2011), we directly visualized, sized and counted total CHIKV particles in culture medium from WT and BST-2$^{-/-}$ MEFs pre-treated with PBS or IFN-β. As expected, the virus titre from NTA was higher than the EPDA titre (compare Fig. 1g, h). However, similar to the EPDA results, expression of BST-2 prevented CHIKV release from MEFs, and IFN-β treatment of WT MEFs further enhanced BST-2-mediated inhibition of CHIKV release with no significant effect on BST-2$^{-/-}$ MEFs (Fig. 1h).

To validate our findings, we treated primary WT and BST-2$^{-/-}$ MEFs with PBS or IFN-β (Fig. 1i) followed by infection. Using NTA, we showed that culture supernatants from BST-2$^{-/-}$ MEFs contained a significantly higher virus titre regardless of IFN-β treatment, whilst supernatants from WT MEFs had a lower virus titre, which was further reduced in the presence of IFN-β (Fig. 1j). Furthermore, expression of BST-2 in primary macrophages was evaluated with confocal microscopy. We showed that CHIKV proteins co-localized with BST-2, as highlighted in the enlarged merged image (Fig. 1k). In macrophages, BST-2 inhibited CHIKV release from infected WT cells (Fig. 1l), although with reduced efficiency compared with MEFs (compare Fig. 1j, l). It should be noted that a modest non-significant decrease in virus release was observed in IFN-treated BST-2$^{-/-}$ cells compared with vehicle-treated BST-2$^{-/-}$ cells (Fig. 1g, h, j, l). This difference could be attributed to a BST-2-independent antiviral effect of IFNs against CHIKV, as has been reported previously (Briolant *et al.*, 2004; Couderc *et al.*, 2008, 2009; Gardner *et al.*, 2012; Partidos *et al.*, 2011; Schilte *et al.*, 2010). These results suggested that BST-2 expression significantly impaired CHIKV 181/25 release.

BST-2-deficient mice are highly susceptible to CHIKV replication at the site of inoculation

The effect of BST-2 on CHIKV replication was tested in a subcutaneous footpad infection assay. Inoculation of WT

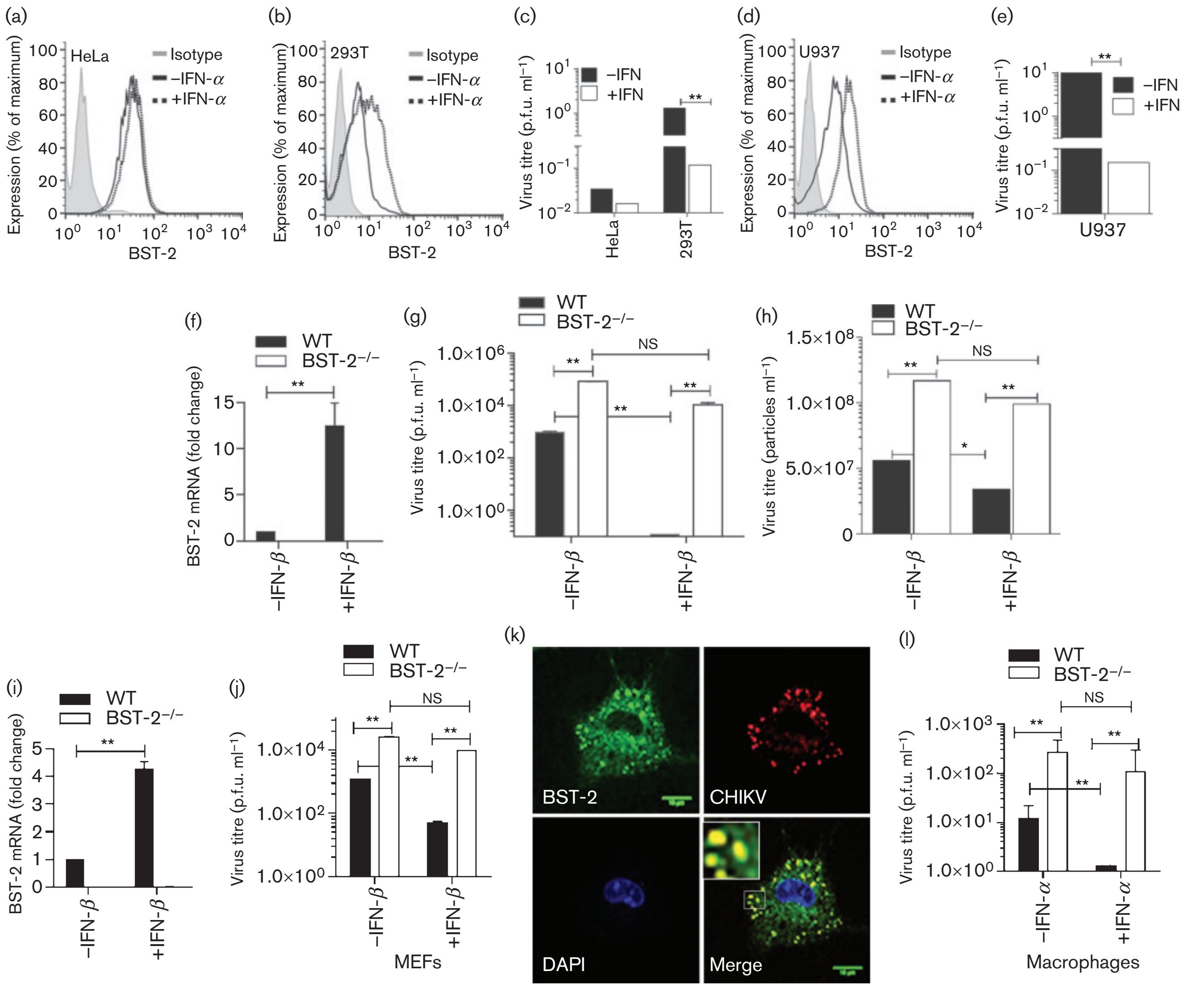

Fig. 1. BST-2 blocks CHIKV release in tissue culture cells. (a, b) Surface BST-2 expression in HeLa (a) and 293T (b) cells cultured in the presence and absence of IFN-α by FACS analysis. (c) EPDA of CHIKV titre released by HeLa and 293T cells cultured in the presence and absence of IFN-α. (d) Surface BST-2 expression in U937 cells treated with or without IFN-α. (e) EPDA of CHIKV titre released by U937 cells treated with or without IFN-α. (f) IFN-β-mediated induction of BST-2 mRNA in immortalized WT MEFs as determined by quantitative real-time (qRT)-PCR. (g) CHIKV titre released by WT and BST-$2^{-/-}$ MEFs cultured in the presence and absence of IFN-β as determined by EPDA. (h) NTA of CHIKV titre released by WT and BST-$2^{-/-}$ MEFs cultured in the presence and absence of IFN-β. (i) Expression of BST-2 mRNA in primary WT MEFs in the presence and absence of IFN-β. (j) CHIKV particles released by primary WT and BST-$2^{-/-}$ MEFs treated with or without IFN-β as determined by NTA. (k) Confocal imaging of BST-2 (green) and CHIKV (red) expression in primary WT macrophages showing co-localization of CHIKV with BST-2. DAPI stains the nucleus and is in blue. Bar, 10 μm. (l) CHIKV titre released by primary WT and BST-$2^{-/-}$ macrophages treated with or without IFN-α as determined by EPDA. There was a significant increase in CHIKV release by BST-$2^{-/-}$ cells compared with WT cells. Treatment with IFNs reduced the amount of released CHIKV. Note that there was a slight decrease in CHIKV released by IFN-treated BST-$2^{-/-}$ cells, which could be attributed to a BST-2-independent IFN effect. For FACS analysis of BST-2 induction by IFN, each cell line was compared with the untreated cells. PCR data were normalized to glyceraldehyde 3-phosphate dehydrogenase (GAPDH) and presented as fold change relative to untreated cells. Virus titre of infectious fluid was determined by either EPDA (p.f.u. ml^{-1}) or NTA (particles ml^{-1}). Experiments were repeated several times with similar results and data presented as the mean ± SD. Significance: *$P<0.05$ and **$P<0.01$; NS, not significant.

and BST-2$^{-/-}$ mice with CHIKV resulted in a significant increase in footpad tissue viral load. Analysis of CHIKV negative-strand RNA in five independent experiments showed that CHIKV replicated more efficiently (~10-fold) in the absence of BST-2 expression (Fig. 2a). Indeed, loss of one BST-2 allele was enough to render mice more susceptible to infection compared with mice with two BST-2 alleles (Fig. 2b). We did not find hind limb swelling in WT or BST-2$^{-/-}$ mice despite the robust virus replication in the footpad of BST-2$^{-/-}$ mice. This finding was not surprising as it had been shown previously that infection with CHIKV 181/25 did not induce hind limb swelling (Gardner *et al.*, 2012). Our results indicated that expression of BST-2 inhibits local CHIKV replication.

Deficiency of BST-2 increases systemic viraemia

Given that the virus titre in the inoculation site in BST-2$^{-/-}$ mice was 10-fold higher than in WT, we hypothesized that the high viral load in BST-2$^{-/-}$ mice would enhance plasma viraemia. EPDA revealed that Vero cells infected with plasma from BST-2$^{-/-}$ mice succumbed to CHIKV-induced cytopathicity at a significantly higher rate than cells infected with BST-2$^{+/-}$ and WT plasma, in that order (Fig. 2c), suggesting that in an equal volume of plasma, BST-2$^{-/-}$ mice produced more infectious particles than BST-2$^{+/-}$ and WT mice ($P<0.01$). To confirm the viral titre result from EPDA, we quantified CHIKV RNA in WT and BST-2$^{-/-}$ cell-free plasma. We detected more CHIKV positive-strand RNA in BST-2$^{-/-}$ plasma compared with WT plasma (Fig. 2d). Our data indicated that BST-2 deficiency enhanced accumulation of viral particles in the bloodstream, suggesting that the higher viraemia in BST-2$^{-/-}$ mice may result in more systemic virus dissemination.

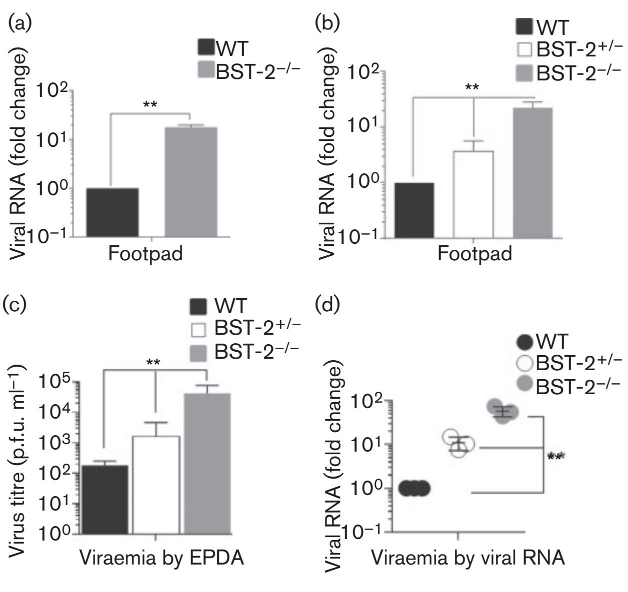

Fig. 2. High inoculation site viral load and plasma viraemia in BST-2-deficient mice. (a, b) WT, BST-2$^{+/-}$ and BST-2$^{-/-}$ mice ($n=3$) were inoculated with 1.5×10^7 p.f.u. CHIKV 181/25 subcutaneously on the hind footpads. Viral load in footpad tissues was determined by qRT-PCR 24 h after infection. (c, d) Plasma viraemia in WT, BST-2$^{+/-}$ and BST-2$^{-/-}$ mice infected with 1.5×10^7 p.f.u. CHIKV 181/25 was determined by EPDA or qRT-PCR 24 h after footpad infection. PCR results were normalized to GAPDH and presented as fold change of WT data. Each data point represents the arithmetic mean ± SD for at least three mice. Significance: **$P<0.01$. Experiments were repeated at least three times with similar results.

BST-2$^{-/-}$ mice have a higher viral load in various peripheral tissues, except the heart

To determine whether higher systemic viraemia in BST-2$^{-/-}$ mice would result in efficient infection of peripheral tissues, we examined the viral load in various lymphoid and non-lymphoid tissues. We found elevated levels of CHIKV RNA in the peripheral blood mononuclear cells (PBMCs), lymph nodes and spleen in BST-2$^{-/-}$ mice compared with their WT counterparts (Fig. 3a–c). Interestingly, the lymph nodes of BST-2$^{-/-}$ mice (Fig. 3b) were overly susceptible to CHIKV, more than the PBMCs (Fig. 3a) and spleen (Fig. 3c). Similar to lymphoid tissues, BST-2$^{-/-}$ mice had a higher viral RNA in the liver (Fig. 3d), lung (Fig. 3e) and stomach (Fig. 3f), but not in the heart (Fig. 3g), compared with WT mice. These data indicated that BST-2 had a tissue-specific effect on CHIKV replication.

BST-2 expression modulates lymphoid tissue tropism in CHIKV infection

Following skin infection, CHIKV spreads to other target tissues/organs within hours, infecting haematopoietic cells and non-haematopoietic cells, albeit to a lower extent (Ozden *et al.*, 2007; Sourisseau *et al.*, 2007). To evaluate the kinetics of the BST-2-dependent response to infection, we infected WT and BST-2$^{-/-}$ mice, and analysed the level of CHIKV RNA in various tissues (Fig. 4a) compared with the level in their respective inoculation site, i.e. footpad tissue (Fig. 4a, inset). The ability of CHIKV to infect different tissues depended on the host genotype. Generally, when compared with the viral load in footpad tissue, the tropism rate of CHIKV to the liver, lung and stomach was similar in both WT and BST-2$^{-/-}$ mice. In the heart, BST-2 deficiency protected mice from CHIKV infection. WT mice had twofold more viral RNA in the heart compared with BST-2$^{-/-}$ mice. Remarkably, the lymph nodes, PBMCs and spleen of BST-2$^{-/-}$ mice were highly permissive to CHIKV replication. To confirm these findings, we quantified the amount of infectious virus in the lymph nodes and spleen by EPDA using tissue homogenates. As expected, loss of BST-2 correlated with increased sensitivity of the lymph nodes and spleen (Fig. 4b, c) to infection. These results suggested that intrinsic BST-2 expression determined permissibility of lymphoid tissues to CHIKV infection.

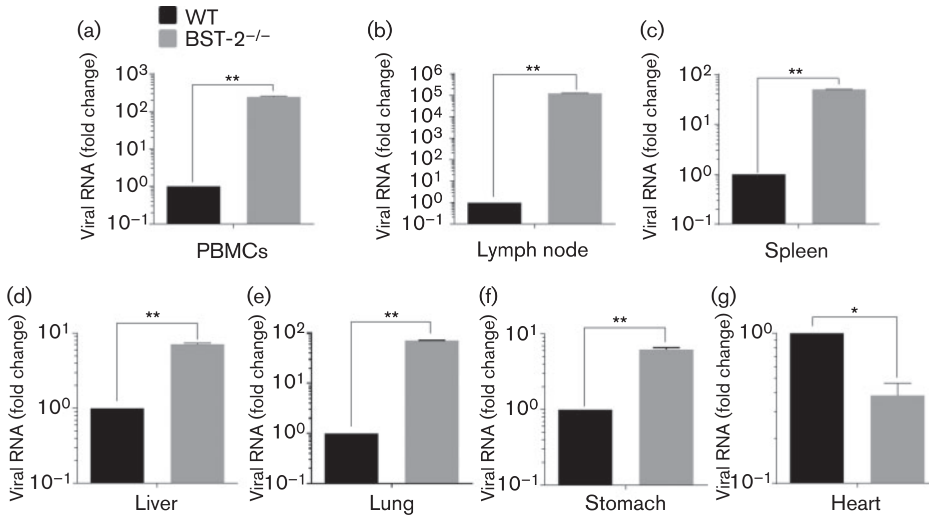

Fig. 3. Increased viral load in multiple tissues of BST-2-deficient mice. (a–g) WT and BST-$2^{-/-}$ mice (n=3) infected with 1.5×10^7 p.f.u. CHIKV 181/25 were euthanized 24 h later. Tissue specimens were collected for RNA extraction and cDNA synthesis. CHIKV replication was evaluated by qRT-PCR using a probe specific for CHIKV nsP1. Viral loads were determined in (a) PBMCs, (b) popliteal lymph nodes, (c) spleen, (d) liver, (e) lung, (f) stomach and (g) heart. Note that viral load in the heart was significantly lower in BST-$2^{-/-}$ mice. Each data point represents the arithmetic mean ± SD for at least three mice normalized to GAPDH and presented as fold change of WT data. Significance: *$P<0.05$*, **$P<0.01$. Data presented are representative of several experiments with similar results.

BST-2 expression at the site of virus inoculation is regulated by CHIKV

To determine if BST-2 expression was altered by CHIKV infection, we evaluated BST-2 mRNA in the footpad tissue of naive and infected WT mice. BST-2 mRNA was elevated in WT footpad tissue 24 h post-infection (Fig. 4d). As BST-2 expression is induced by IFN-α, we examined IFN-α mRNA expression in the footpad tissue. BST-$2^{-/-}$ mice have higher basal IFN-α in their footpad tissue than WT mice (Fig. 4e). However, upon infection, CHIKV induced IFN-α mRNA expression in WT footpad tissue, but not in BST-$2^{-/-}$ footpad tissue (Fig. 4f), supporting a previous report that BST$2^{-/-}$ mice produced less type I IFN than their WT control following viral infection (Swiecki *et al.*, 2012). The increase in footpad tissue IFN-α correlated with upregulation of BST-2 mRNA, indicating that CHIKV regulation of IFN-α was partly dependent on BST-2 expression.

Analysis of differentially expressed inflammatory cytokines and chemokines

Infection with CHIKV elicits a robust inflammatory response (Hoarau *et al.*, 2010; Wauquier *et al.*, 2011) resulting in alteration in the host transcriptome. Such alterations are likely determinants of the fate of infection, with regard to immune responses and disease outcome. To determine if the absence of BST-2 expression modulated inflammatory cytokines at the site of inoculation, we conducted targeted mouse inflammatory cytokine and receptor PCR array analysis using footpad tissue from naive and infected mice. Out of 86 genes evaluated (Fig. 5a), 60 genes were commonly upregulated more than twofold in WT and BST-$2^{-/-}$ mice, and 17 genes were commonly downregulated (Fig. 5b). Nicotinamide phosphoribosyltransferase (NAMPT, also known as visfatin) was significantly downregulated in WT mice compared with BST-$2^{-/-}$ mice (Fig. 5b). We found that IFN-γ and CD40L were the most highly CHIKV-induced genes in WT mice compared with BST-$2^{-/-}$ mice. We validated IFN-γ and CD40L expression by quantitative real-time (qRT)-PCR. Basal IFN-γ mRNA was higher in BST-$2^{-/-}$ footpad tissue compared with WT footpad tissue (Fig. 5d), but CHIKV suppressed IFN-γ expression in BST-$2^{-/-}$ footpad tissue (Fig. 5e). The level of CD40L in naive footpad tissue was similar between WT and BST-$2^{-/-}$ footpad tissue (Fig. 5f). However, CD40L mRNA significantly decreased in infected BST-$2^{-/-}$ footpad tissue (Fig. 5g). These results indicated that differences in early immune responses between WT and BST-$2^{-/-}$ mice may have been linked to their different responses to infection with CHIKV.

Expression of innate immunity genes in the lymph node draining the site of CHIKV delivery is BST-2 dependent

Here, we analysed the expression of IFN-γ, CD40L, IFN-α and BST-2 in the draining lymph nodes of WT and BST-$2^{-/-}$ mice. The basal level of IFN-γ present in BST-$2^{-/-}$ lymph nodes was significantly higher than that in the WT

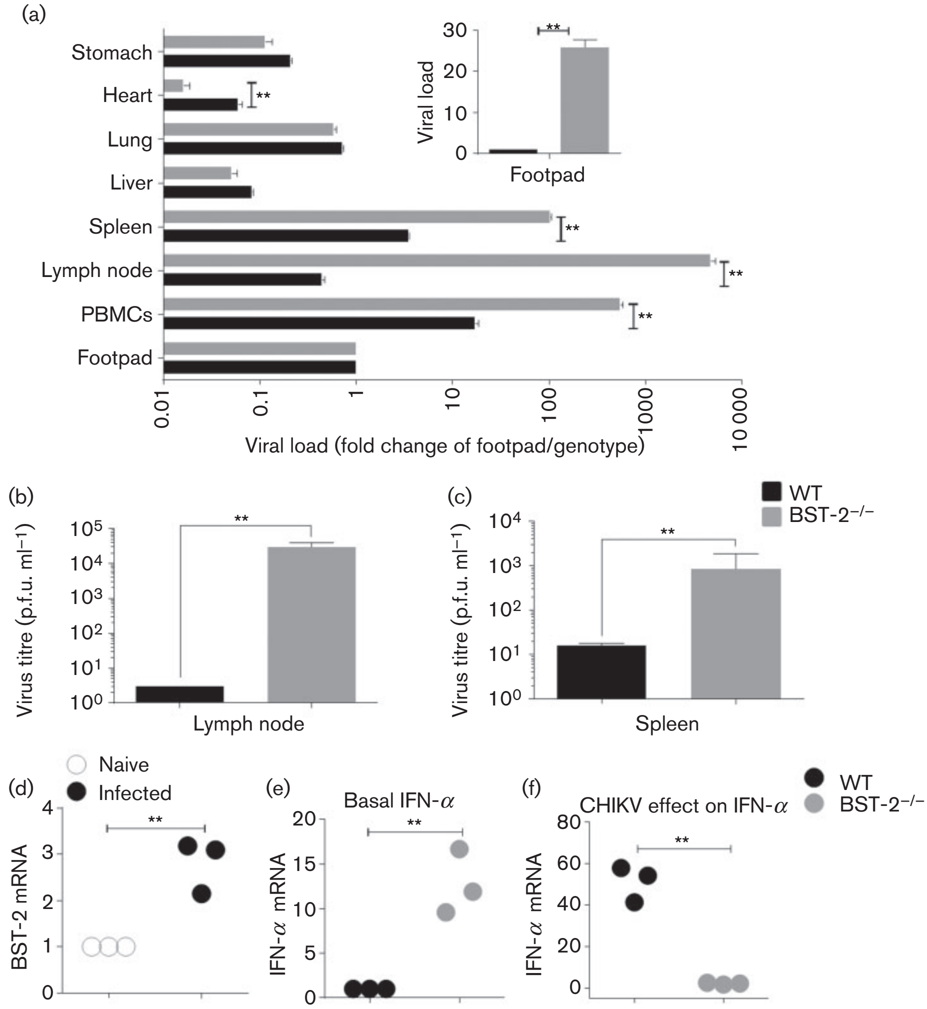

Fig. 4. BST-2 protects lymphoid tissues from efficient CHIKV infection. (a) WT and BST-$2^{-/-}$ mice (n=3) were inoculated with 1.5×10^7 p.f.u. CHIKV 181/25 on the footpad. Mice were euthanized 24 h later. RNA extracted from the footpads, PBMCs, lymph nodes, spleen, liver, lung, heart and stomach was subjected to qRT-PCR analysis with a probe specific for CHIKV nsP1. After normalization to GAPDH, viral load in each tissue (amount of virus detected in a specific tissue) was compared with the respective footpad viral load (inset) and presented as fold change of footpad data. (b) Lymph node and (c) spleen homogenates were titrated onto replicate Vero cell cultures in 48-well plates for titre determination by EPDA. Homogenate viral load is presented as p.f.u. ml^{-1}. (d) Footpad tissue RNA from WT mice was used for PCR determination of the level of BST-2 mRNA expressed in uninfected and infected footpad tissues. Data are presented as fold change of uninfected mRNA. (e) Footpad tissue RNA from WT and BST-$2^{-/-}$ mice was used for qRT-PCR determination of basal IFN-α mRNA expressed in uninfected footpad tissue. Data were normalized to GAPDH and presented as fold change of WT. (f) Footpad tissue RNA from WT and BST-$2^{-/-}$ mice was used to evaluate the effect of CHIKV on IFN-α expression. Data for each mouse genotype was normalized to GAPDH and presented as fold change of uninfected footpad tissue (e). Bar, SD. Significance: **$P<0.01$. Data presented are representative of several experiments with similar results.

controls (Fig. 6a). However, CHIKV suppressed IFN-γ expression in BST-$2^{-/-}$ lymph nodes (Fig. 6b) as well as IFN-γ production in BST-$2^{-/-}$ plasma (Fig. 6c). Likewise, basal CD40L expression (Fig. 6d, e) was higher in BST-$2^{-/-}$ lymph nodes, but CHIKV markedly reduced CD40L in BST-$2^{-/-}$ mice compared with the WT (Fig. 6f–g).

BST-2 expression in draining lymph nodes of WT mice was downregulated by CHIKV at both the mRNA (Fig. 6h) and protein (Fig. 6i) levels. Additionally, IFN-α mRNA was higher in naive BST-$2^{-/-}$ lymph nodes compared with WT lymph nodes (Fig. 6j). However, CHIKV significantly suppressed IFN-α expression in BST-$2^{-/-}$ lymph nodes, but not in WT (Fig. 6k). These results clearly indicated that BST-2 was critical for the protection of lymphoid tissues against CHIKV infection by promoting some early innate immune response events following infection.

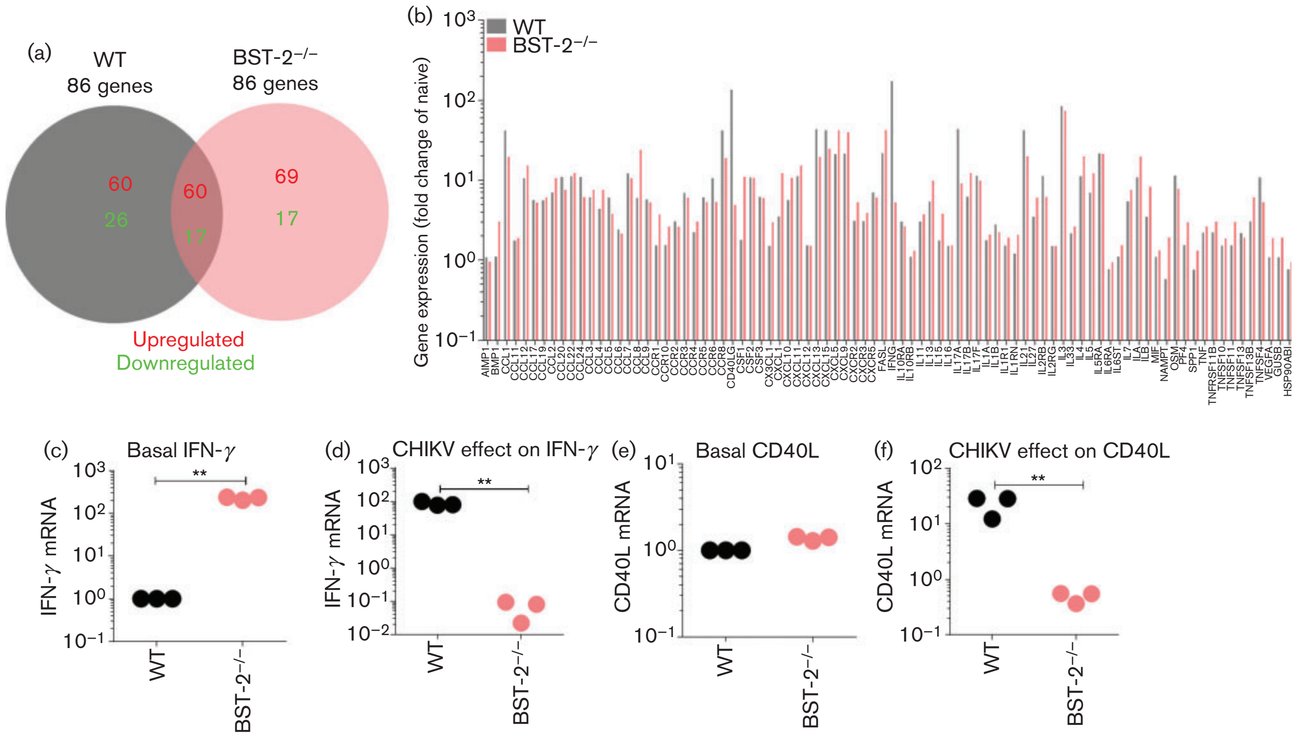

Fig. 5. Gene expression profile of inflammatory cytokines and receptors analysed by PCR array analysis and qRT-PCR. (a) RNA from footpad tissue described in Fig. 4(a) was used in RT^2 Profiler PCR Array analysis of mouse inflammatory cytokines and receptors (PAMM-011A) for evaluation of the expression of a focused panel of genes. Data analysis was performed using the $\Delta\Delta C_t$ method according to the manufacturer's protocol (SABiosciences) to generate fold change expression. For each gene, fold changes were calculated as the difference in gene expression between naive footpads and infected footpads. Fold change values of $\geqslant$2.0 and $<$2.0 were chosen as cut-off values representing up- and downregulation, respectively. The Venn diagram depicts the numbers of genes up- or downregulated in WT (grey) and BST-$2^{-/-}$ (pink) footpads. The overlap represents the number and type (up- or downregulation) of transcriptional modifications. Upregulation, red; downregulation, green. (b) Fold change in gene expression depicting levels of CHIKV-mediated transcriptional alterations. Data represent fold change in the mRNA expression levels of cytokines, inflammatory regulators, cytokine receptors, chemokines, and chemokine receptors expressed in WT and BST-$2^{-/-}$ in response to 24 h CHIKV infection ($P<0.05$). (c, d) Validation of IFN-γ expression by qRT-PCR using footpad RNA from WT and BST-$2^{-/-}$ mice that were not infected or infected with CHIKV, respectively. Data were normalized to GAPDH and presented as fold change of WT or naive. (e, f) RNA from WT and BST-$2^{-/-}$ mice isolated from naive and infected footpad tissue was used to validate CD40L mRNA expression. Data were normalized to GAPDH and presented as fold change of WT or naive. Bar, SD. Significance: $^{**}P<0.01$. Data presented are representative of several experiments with similar results.

DISCUSSION

In this study, we conducted *in vivo* experiments to improve our understanding of the role of BST-2 in CHIKV replication and host defence. We extended our prior work on the effect of BST-2 expression in the release of CHIKV virus-like particles (Jones *et al.*, 2013b) and demonstrated that infectious CHIKV 181/25 is susceptible to the effect of BST-2 in human cells (Fig. 1c, e). We confirmed that infectious CHIKV co-localizes with BST-2, and that BST-2 inhibits release of infectious CHIKV from infected MEFs and macrophages (Fig. 1g, h, j, l).

It has been shown previously that CHIKV 181/25, which does not cause serious inflammatory disease, is non-lethal in mice (Gardner *et al.*, 2012). In the present study, we did not observe lethality as we concluded all studies at 24 h. Despite the lack of lethality, BST-$2^{-/-}$ mice were highly susceptible to CHIKV replication at the site of inoculation. Indeed, viral load in the footpad tissue of infected BST-$2^{-/-}$ mice was 10-fold higher than that in WT controls (Fig. 2a). This point was further elucidated by the fact that heterozygote mice (BST-$2^{+/-}$) were more susceptible to inoculation site CHIKV replication compared with WT mice (Fig. 2e). Increased inoculation site viral load in BST-$2^{-/-}$ mice correlated directly with amplified systemic viraemia 24 h post-infection, indicating that BST-2 mediates release of virions into the extracellular milieu *in vivo*.

The high extracellular virus titre in BST-$2^{-/-}$ mice corresponded to systemic dissemination and elevated viral

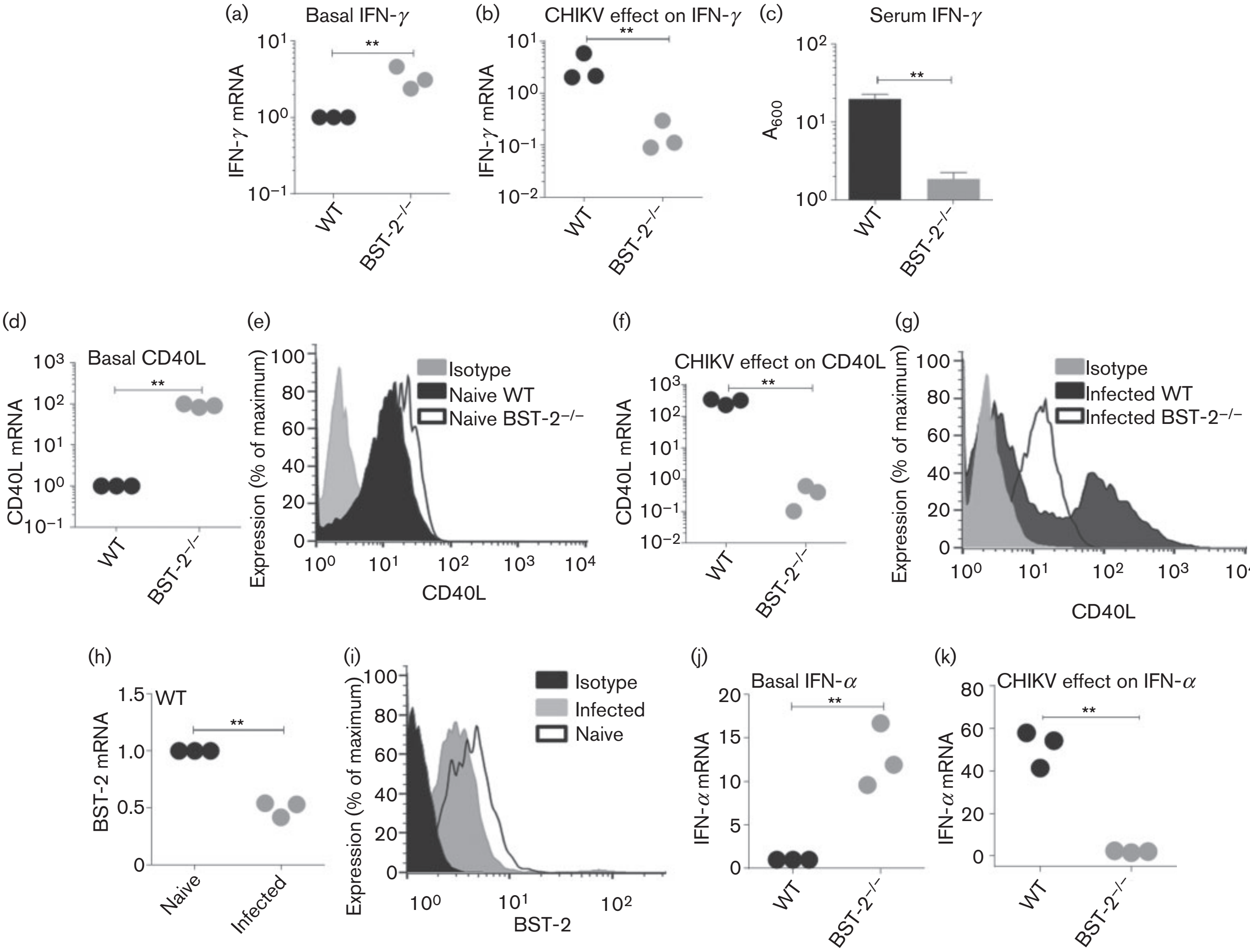

Fig. 6. CHIKV-associated downregulation of gene expression in the lymph nodes of BST-$2^{-/-}$ mice. (a, b) Analysis of IFN-γ mRNA from lymph nodes of naive and infected mice. Data were normalized to GAPDH and presented as fold change of uninfected lymph nodes. (c) Serum IFN-γ level from infected mice analysed by ELISA. Each data point was normalized to naive serum for background subtraction and data presented as raw absorbance. (d) Analysis of basal CD40L mRNA presented as fold change of WT mRNA. (e) Surface expression of CD40L in lymph nodes of WT and BST-$2^{-/-}$ naive mice elucidated by FACS analysis. (f) Analysis of CD40L mRNA in CHIKV-infected lymph nodes presented as fold change of naive lymph nodes. (g) Surface expression of CD40L in infected lymph nodes of WT and BST-$2^{-/-}$ mice elucidated by FACS analysis. (h) qRT-PCR of BST-2 mRNA in naive and infected WT lymph nodes presented as fold change of naive lymph nodes. (i) Surface expression of BST-2 in lymph nodes of WT naive and infected mice analysed by FACS. (j) IFN-α mRNA in WT and BST-$2^{-/-}$ lymph nodes presented as fold change of WT lymph nodes. (k) qRT-PCR analysis of IFN-α in infected lymph nodes presented as fold change of uninfected lymph nodes. qRT-PCR data were normalized to GAPDH and presented as fold change. Bar, SD. Significance: $^{**}P<0.01$. Experiments were repeated over three times with similar results.

load in distant tissues. BST-2 expression was found to be particularly important in protecting lymphoid tissues from CHIKV tropism. This could, in part, explain why lymphoid tissues in WT mice are relatively less susceptible to CHIKV infection, as has been reported previously (Das *et al.*, 2010; Her *et al.*, 2010; Labadie *et al.*, 2010; Sourisseau *et al.*, 2007). Interestingly, not all tissues lacking BST-2 are susceptible to high CHIKV infection. We found that loss of BST-2 protects the heart from CHIKV replication because levels of CHIKV negative-strand RNA present in the heart of WT mice were higher compared with their BST-$2^{-/-}$ littermates, suggesting that BST-2 plays a tissue/cell-type-dependent role against CHIKV infection.

Evaluation of gene expression following CHIKV infection revealed that CHIKV altered the levels of inflammatory cytokines and chemokines in a BST-2-dependent manner. We found that levels of NAMPT were downregulated in WT mice infected with CHIKV and slightly upregulated (1.9-fold) in CHIKV-infected BST-$2^{-/-}$ mice. The finding in WT mice supports a previous report which showed that

CHIKV infection downregulated NAMPT expression (Thio *et al.*, 2013). NAMPT is located both intracellularly and extracellularly. Inside the cell, NAMPT functions as a rate-limiting enzyme in the NAD^+ salvage pathway (Garten *et al.*, 2009). Extracellular NAMPT is suggested to have enzymic and pro-inflammatory activities (Romacho *et al.*, 2009; Wang *et al.*, 2009). NAMPT has been implicated in various pathological conditions, such as rheumatoid arthritis (Otero *et al.*, 2006). In HIV-1-infected cells, suppression of NAMPT expression by miR-182 was shown to be involved in Tat-induced HIV-1 long-terminal repeat transactivation (Chen *et al.*, 2013). In addition, NAMPT inhibited infection by HIV-1 using the CCR5 co-receptor, but enhanced infection by CXCR4 (Van den Bergh *et al.*, 2012). The effect of NAMPT on HIV-1 replication suggests that NAMPT has the potential to selectively modulate viral pathogenesis. The differential effect of CHIKV on NAMPT levels in the presence and absence of BST-2 is interesting and indicative of BST-2-mediated regulation of NAMPT.

Another significant finding from our study was the suppression of IFN-α and IFN-γ by CHIKV in BST-$2^{-/-}$ mice. Previous studies indicated that BST-2 blocks secretion of IFN-α by plasmacytoid dendritic cells (Cao *et al.*, 2009), and we found mRNAs encoding IFN-α and IFN-γ to be higher in BST$2^{-/-}$ mouse footpad and lymph node tissues at baseline compared with WT mice. The reason behind the increase in steady-state levels of IFN-α and IFN-γ in uninfected BST-$2^{-/-}$ mice is unclear, but could be attributed to compensatory mechanisms for immune regulation in the absence of BST-2. Upon infection, however, CHIKV downmodulates the expression of these IFNs, supporting a previous finding that BST$2^{-/-}$ mice produced less IFN-α than their WT controls following systemic viral infections (Swiecki *et al.*, 2012). As type I and II IFNs are critical for the control of CHIKV infection (Briolant *et al.*, 2004; Couderc *et al.*, 2008, 2009; Gardner *et al.*, 2012; Partidos *et al.*, 2011; Schilte *et al.*, 2010; Wauquier *et al.*, 2011), our finding implies that the inability of BST-$2^{-/-}$ mice to produce IFNs upon infection with CHIKV may contribute to their enhanced susceptibility to the virus. Furthermore, the absence of IFN mRNA and protein in BST-$2^{-/-}$ mice is suggestive of the involvement of BST-2 in the regulation of IFN during CHIKV infection. This point is intriguing as BST-2 has the potential to activate antigen-presenting cells (APCs), as described previously (Blasius *et al.*, 2006). In this case, BST-2 expressed in WT cells may function to sense CHIKV and prime target cells in response to CHIKV, with a resultant increase in cytokine secretion.

In addition to suppression of IFNs in BST-$2^{-/-}$ mice, we found that expression of CD40L in BST-$2^{-/-}$ mice was suppressed markedly by CHIKV. CD40L is a type II transmembrane inflammatory regulator expressed in many cell types, including $CD4^+$ T-cells, monocytes, macrophages, endothelial cells and platelets (Rizvi *et al.*, 2008). As with IFNs, an enhanced basal CD40L level in BST-$2^{-/-}$ mice could be a compensatory event for the generation of optimal immune activation. However, CHIKV was able to downmodulate CD40L in BST-$2^{-/-}$ mice. The reduction of CD40L in infected BST-$2^{-/-}$ mice could stem from the inability of BST-$2^{-/-}$ mice to efficiently sense incoming CHIKV, resulting in inefficient APC activation, suboptimal CD40–CD40L interaction and secretion of cytokines, including IFN-γ. Indeed, BST-2 has been shown recently to act as a pattern recognition receptor that senses HIV-1 and activates the NFκB signalling pathway, culminating in secretion of antiviral factors (Galão *et al.*, 2012). A previous study implicated reduced CD40L and IFN-α expression in the pathogenesis of chronic CHIKV-induced arthritis (Malvy *et al.*, 2009). CD40L can regulate the immune response (Mackey *et al.*, 1998) either by (i) activating APCs to express co-stimulatory molecules including B7 (CD80 and CD86), (ii) generating cytotoxic T-lymphocytes against virus-infected cells or (iii) stimulating IFN-γ production.

The observed suppression of expression of IFN-α, IFN-γ and CD40L at the site of virus inoculation and in the popliteal lymph node draining the site of infection in BST-$2^{-/-}$ mice signifies that BST-2 regulates these genes. Deficiency of BST-2 expression results in suppression of genes that have been shown to be effective against CHIKV. Particularly affected may be genes that are involved in B-cell differentiation, optimal immunoglobulin isotype switching and antiviral activity. It is therefore possible that (i) CHIKV may more efficiently evade T-cell-dependent immunoglobulin (IgA and IgG) responses in the absence of CD40L gene expression (Whitmire *et al.*, 1999), (ii) the presence of CD40L in WT mice may function to stimulate production of IFN-γ, which in turn protects cells from CHIKV infection, as has been reported for HIV (Fan *et al.*, 1994; Kornbluth *et al.*, 1989), and (iii) tethering of CHIKV at the cell surface by BST-2 (Jones *et al.*, 2013b) may not only prevent CHIKV release, but also mediate clearance of the virus and its reservoirs through antibody-dependent cell-mediated cytotoxicity, as has been shown for HIV-infected cells (Arias *et al.*, 2014; Veillette *et al.*, 2014). Overall, our study has contributed to defining the effect of BST-2 on CHIKV replication and host protection. Further studies will be necessary to determine whether BST-2 is operative on more virulent CHIKV strains, assess the role of BST-2 in CHIKV disease and elaborate on the role of CHIKV-modulated genes in CHIKV pathogenesis in the absence of BST-2.

METHODS

Animals. WT and BST-$2^{-/-}$ mice (Jones *et al.*, 2013a; Swiecki *et al.*, 2012) were inoculated on the hind footpad with CHIKV 181/25 (1.5×10^7 p.f.u.). This dose was used because lower doses did not produce detectable CHIKV in distal tissues other than the inoculation site in WT mice. As we were focused on early events, comparisons between WT and BST-$2^{-/-}$ mice could not be accomplished with low viral dose. Mice were bled for plasma and PBMCs 24 h later and sacrificed. At necropsy, tissues were collected for viral load determination. When indicated, single cells from lymph nodes were analysed for surface BST-2 and CD40L expression. Experiments involving mice were approved by the University of Iowa Animal Care and Use Committee.

Cells. Vero, 293T, HeLa, U937 and MEF cells from WT and BST-2$^{-/-}$ mice [all from the American Type Culture Collection (ATCC)] were maintained in Dulbecco's modified Eagle's medium or as recommended by the ATCC.

Virus stock. CHIKV strain 181/25 (Levitt *et al.*, 1986) was inoculated onto Vero cells. Upon appearance of cytopathic effects, culture supernatants were harvested, clarified (1000 ***g*** for 5 min), aliquoted and stored (−80 °C) until titres were determined by EPDA on Vero cells.

Virus replication. Monolayers of cell of interest in 48-well plates were inoculated with CHIKV (m.o.i. 0.1), allowed to adsorb (1 h at 35 °C), washed, and fresh medium was added to each well. Cells were incubated at 37 °C for 24 h. Infectious fluids were used for titre determination.

EPDA. Serial dilutions of infectious fluids were inoculated onto replicate Vero cells. Cells were monitored daily and on day 5 post-inoculation the number of cells infected was determined for each virus dilution by examining cells for cytopathicity. The end-point (day 5 for our assays) was calculated from the data and expressed as $TCID_{50}$. The $TCID_{50}$ was expressed as p.f.u. ml^{-1} by multiplying the $TCID_{50}$ titre by 0.7 (Mills *et al.*, 1971).

NTA. NTA is a single-particle detection system that allows measurement of total virus concentration (infectious and non-infectious particles) in liquid suspension. Clarified supernatants from infected cells were injected into an NTA NS300 (NanoSight) sample chamber using a syringe and particle movement was video-captured. For each experiment, mean particle number was counted from 20 frames of videos from measurements per sample recorded over 30 s with a mean error of 2 %. Measurements were taken at room temperature. Data were analysed using NTA 2.3 software. Supernatant virus titre was reported as particles ml^{-1}. All buffers were filtered through 0.02 μm filters and checked for absence of particles before use.

Protein analysis by FACS and ELISA. Confocal imaging, FACS and ELISA analysis were performed as described previously (Jones *et al.*, 2012, 2013a, b) with antibodies against IFN-γ, BST-2 and CD40L (eBioscience), and appropriate IgG.

RNA isolation, and viral and host gene mRNA quantification. RNA was isolated from cells/tissues with the RNeasy Mini kit (Qiagen) and from plasma with the QIAamp Viral RNA kit (Qiagen). Equivalent amounts of RNA treated with DNase I (Qiagen) were reverse transcribed with a high-capacity cDNA reverse transcription kit (ABI) and amplified with target-specific primers (Jones & Okeoma, 2013; Mehta *et al.*, 2012).

Microscopy. As we described previously, macrophages plated on coverslips were infected with CHIKV for 24 h. Cells were stained with anti-mouse CHIKV polyclonal antibody, anti-BST-2 antibody and appropriate secondary antibodies (Jones *et al.*, 2013b). Confocal images were acquired using a Zeiss 710 confocal microscope.

PCR array analysis. Gene expression was analysed using RT^2 Profiler PCR Array mouse inflammatory cytokines and receptors and RT^2 Real-Time SYBR Green/PCR Master Mix (SABiosciences). cDNA synthesized from 1 μg total footpad RNA was amplified in the presence of 86 specific primers coated in 96-well microtitre plates on an ABI 7500 Fast Real-Time PCR System. Data were analysed by the web-based Analysis Template provided by SABiosciences.

Statistics. Statistical analysis was performed by paired Student's *t*-test.

ACKNOWLEDGEMENTS

This work was supported by funds from the Department of Microbiology of the University of Iowa, National Cancer Institute of the National Institutes of Health (P30CA086862) and National Institutes of Health T32 (AI007511). Publication of this paper was made possible through core services from the University of Iowa Central Microscopy Research Facility. We thank Marisa Madison, Alexander Canfield and Bryson Okeoma of the University of Iowa for help with ELISA, EPDA and constructive criticism, respectively.

REFERENCES

Arias, J. F., Heyer, L. N., von Bredow, B., Weisgrau, K. L., Moldt, B., Burton, D. R., Rakasz, E. G. & Evans, D. T. (2014). Tetherin antagonism by Vpu protects HIV-infected cells from antibody-dependent cell-mediated cytotoxicity. *Proc Natl Acad Sci U S A* **111**, 6425–6430.

Blasius, A. L., Giurisato, E., Cella, M., Schreiber, R. D., Shaw, A. S. & Colonna, M. (2006). Bone marrow stromal cell antigen 2 is a specific marker of type I IFN-producing cells in the naive mouse, but a promiscuous cell surface antigen following IFN stimulation. *J Immunol* **177**, 3260–3265.

Briolant, S., Garin, D., Scaramozzino, N., Jouan, A. & Crance, J. M. (2004). *In vitro* inhibition of Chikungunya and Semliki Forest viruses replication by antiviral compounds: synergistic effect of interferon-alpha and ribavirin combination. *Antiviral Res* **61**, 111–117.

Cao, W., Bover, L., Cho, M., Wen, X., Hanabuchi, S., Bao, M., Rosen, D. B., Wang, Y. H., Shaw, J. L. & other authors (2009). Regulation of TLR7/9 responses in plasmacytoid dendritic cells by BST2 and ILT7 receptor interaction. *J Exp Med* **206**, 1603–1614.

Chen, X. Y., Zhang, H. S., Wu, T. C., Sang, W. W. & Ruan, Z. (2013). Down-regulation of NAMPT expression by miR-182 is involved in Tat-induced HIV-1 long terminal repeat (LTR) transactivation. *Int J Biochem Cell Biol* **45**, 292–298.

Couderc, T., Chrétien, F., Schilte, C., Disson, O., Brigitte, M., Guivel-Benhassine, F., Touret, Y., Barau, G., Cayet, N. & other authors (2008). A mouse model for Chikungunya: young age and inefficient type-I interferon signaling are risk factors for severe disease. *PLoS Pathog* **4**, e29.

Couderc, T., Khandoudi, N., Grandadam, M., Visse, C., Gangneux, N., Bagot, S., Prost, J. F. & Lecuit, M. (2009). Prophylaxis and therapy for Chikungunya virus infection. *J Infect Dis* **200**, 516–523.

Das, T., Jaffar-Bandjee, M. C., Hoarau, J. J., Krejbich Trotot, P., Denizot, M., Lee-Pat-Yuen, G., Sahoo, R., Guiraud, P., Ramful, D. & Robin, S. (2010). Chikungunya fever: CNS infection and pathologies of a re-emerging arbovirus. *Prog Neurobiol* **91**, 121–129.

Douglas, J. L., Gustin, J. K., Viswanathan, K., Mansouri, M., Moses, A. V. & Früh, K. (2010). The great escape: viral strategies to counter BST-2/tetherin. *PLoS Pathog* **6**, e1000913.

Du, S., Kendall, K., Morris, S. & Sweet, C. (2010). Measuring number-concentrations of nanoparticles and viruses in liquids on-line. *J Chem Technol Biotechnol* **85**, 1223–1228.

Fan, S. X., Turpin, J. A., Aronovitz, J. R. & Meltzer, M. S. (1994). Interferon-gamma protects primary monocytes against infection with human immunodeficiency virus type 1. *J Leukoc Biol* **56**, 362–368.

Filipe, V., Jiskoot, W. & Hawe, A. (2011). Understanding virus preparations using nanoscale particle characterization. *BioProcess Int* **9**, 44–51.

Galão, R. P., Le Tortorec, A., Pickering, S., Kueck, T. & Neil, S. J. (2012). Innate sensing of HIV-1 assembly by Tetherin induces NFκB-dependent proinflammatory responses. *Cell Host Microbe* **12**, 633–644.

Gardner, C. L., Burke, C. W., Higgs, S. T., Klimstra, W. B. & Ryman, K. D. (2012). Interferon-alpha/beta deficiency greatly exacerbates arthritogenic disease in mice infected with wild-type chikungunya virus but not with the cell culture-adapted live-attenuated 181/25 vaccine candidate. *Virology* **425**, 103–112.

Garten, A., Petzold, S., Körner, A., Imai, S. i. & Kiess, W. (2009). Nampt: linking NAD biology, metabolism and cancer. *Trends Endocrinol Metab* **20**, 130–138.

Her, Z., Malleret, B., Chan, M., Ong, E. K., Wong, S. C., Kwek, D. J., Tolou, H., Lin, R. T., Tambyah, P. A. & other authors (2010). Active infection of human blood monocytes by Chikungunya virus triggers an innate immune response. *J Immunol* **184**, 5903–5913.

Hoarau, J. J., Jaffar Bandjee, M. C., Krejbich Trotot, P., Das, T., Li-Pat-Yuen, G., Dassa, B., Denizot, M., Guichard, E., Ribera, A. & other authors (2010). Persistent chronic inflammation and infection by Chikungunya arthritogenic alphavirus in spite of a robust host immune response. *J Immunol* **184**, 5914–5927.

Jones, P. H. & Okeoma, C. M. (2013). Phosphatidylinositol 3-kinase is involved in Toll-like receptor 4-mediated BST-2/tetherin regulation. *Cell Signal* **25**, 2752–2761.

Jones, P. H., Mehta, H. V., Maric, M., Roller, R. J. & Okeoma, C. M. (2012). Bone marrow stromal cell antigen 2 (BST-2) restricts mouse mammary tumor virus (MMTV) replication *in vivo*. *Retrovirology* **9**, 10.

Jones, P. H., Mahauad-Fernandez, W. D., Madison, M. N. & Okeoma, C. M. (2013a). BST-2/tetherin is overexpressed in mammary gland and tumor tissues in MMTV-induced mammary cancer. *Virology* **444**, 124–139.

Jones, P. H., Maric, M., Madison, M. N., Maury, W., Roller, R. J. & Okeoma, C. M. (2013b). BST-2/tetherin-mediated restriction of chikungunya (CHIKV) VLP budding is counteracted by CHIKV non-structural protein 1 (nsP1). *Virology* **438**, 37–49.

Kornbluth, R. S., Oh, P. S., Munis, J. R., Cleveland, P. H. & Richman, D. D. (1989). Interferons and bacterial lipopolysaccharide protect macrophages from productive infection by human immunodeficiency virus *in vitro*. *J Exp Med* **169**, 1137–1151.

Labadie, K., Larcher, T., Joubert, C., Mannioui, A., Delache, B., Brochard, P., Guigand, L., Dubreil, L., Lebon, P. & other authors (2010). Chikungunya disease in nonhuman primates involves long-term viral persistence in macrophages. *J Clin Invest* **120**, 894–906.

Levitt, N. H., Ramsburg, H. H., Hasty, S. E., Repik, P. M., Cole, F. E., Jr & Lupton, H. W. (1986). Development of an attenuated strain of chikungunya virus for use in vaccine production. *Vaccine* **4**, 157–162.

Liberatore, R. A. & Bieniasz, P. D. (2011). Tetherin is a key effector of the antiretroviral activity of type I interferon *in vitro* and *in vivo*. *Proc Natl Acad Sci U S A* **108**, 18097–18101.

Lopez, L. A., Yang, S. J., Exline, C. M., Rengarajan, S., Haworth, K. G. & Cannon, P. M. (2012). Anti-tetherin activities of HIV-1 Vpu and Ebola virus glycoprotein do not involve removal of tetherin from lipid rafts. *J Virol* **86**, 5467–5480.

Mackey, M. F., Barth, R. J., Jr & Noelle, R. J. (1998). The role of CD40/CD154 interactions in the priming, differentiation, and effector function of helper and cytotoxic T cells. *J Leukoc Biol* **63**, 418–428.

Malvy, D., Ezzedine, K., Mamani-Matsuda, M., Autran, B., Tolou, H., Receveur, M. C., Pistone, T., Rambert, J., Moynet, D. & Mossalayi, D. (2009). Destructive arthritis in a patient with chikungunya virus infection with persistent specific IgM antibodies. *BMC Infect Dis* **9**, 200.

Mehta, H. V., Jones, P. H., Weiss, J. P. & Okeoma, C. M. (2012). IFN-α and lipopolysaccharide upregulate APOBEC3 mRNA through different signaling pathways. *J Immunol* **189**, 4088–4103.

Mills, J., Chanock, V. & Chanock, R. M. (1971). Temperature-sensitive mutants of influenza virus. I. Behavior in tissue culture and in experimental animals. *J Infect Dis* **123**, 145–157.

Neil, S. J., Zang, T. & Bieniasz, P. D. (2008). Tetherin inhibits retrovirus release and is antagonized by HIV-1 Vpu. *Nature* **451**, 425–430.

Olagnier, D., Scholte, F. E., Chiang, C., Albulescu, I. C., Nichols, C., He, Z., Lin, R., Snijder, E. J., van Hemert, M. J. & Hiscott, J. (2014). Inhibition of dengue and chikungunya virus infections by RIG-I-mediated type I IFN-independent stimulation of the innate antiviral response. *J Virol* **88**, 4180–4194.

Otero, M., Lago, R., Gomez, R., Lago, F., Dieguez, C., Gómez-Reino, J. J. & Gualillo, O. (2006). Changes in plasma levels of fat-derived hormones adiponectin, leptin, resistin and visfatin in patients with rheumatoid arthritis. *Ann Rheum Dis* **65**, 1198–1201.

Ozden, S., Huerre, M., Riviere, J. P., Coffey, L. L., Afonso, P. V., Mouly, V., de Monredon, J., Roger, J. C., El Amrani, M. & other authors (2007). Human muscle satellite cells as targets of Chikungunya virus infection. *PLoS ONE* **2**, e527.

Partidos, C. D., Weger, J., Brewoo, J., Seymour, R., Borland, E. M., Ledermann, J. P., Powers, A. M., Weaver, S. C., Stinchcomb, D. T. & Osorio, J. E. (2011). Probing the attenuation and protective efficacy of a candidate chikungunya virus vaccine in mice with compromised interferon (IFN) signaling. *Vaccine* **29**, 3067–3073.

Pham, T. N., Lukhele, S., Hajjar, F., Routy, J. P. & Cohen, E. A. (2014). HIV Nef and Vpu protect HIV-infected $CD4^+$ T cells from antibody-mediated cell lysis through down-modulation of CD4 and BST2. *Retrovirology* **11**, 15.

Pialoux, G., Gaüzère, B. A., Jauréguiberry, S. & Strobel, M. (2007). Chikungunya, an epidemic arbovirosis. *Lancet Infect Dis* **7**, 319–327.

Powers, A. M. & Logue, C. H. (2007). Changing patterns of chikungunya virus: re-emergence of a zoonotic arbovirus. *J Gen Virol* **88**, 2363–2377.

Radoshitzky, S. R., Dong, L., Chi, X., Clester, J. C., Retterer, C., Spurgers, K., Kuhn, J. H., Sandwick, S., Ruthel, G. & other authors (2010). Infectious Lassa virus, but not filoviruses, is restricted by BST-2/tetherin. *J Virol* **84**, 10569–10580.

Rizvi, M., Pathak, D., Freedman, J. E. & Chakrabarti, S. (2008). CD40–CD40 ligand interactions in oxidative stress, inflammation and vascular disease. *Trends Mol Med* **14**, 530–538.

Romacho, T., Azcutia, V., Vázquez-Bella, M., Matesanz, N., Cercas, E., Nevado, J., Carraro, R., Rodríguez-Mañas, L., Sánchez-Ferrer, C. F. & Peiró, C. (2009). Extracellular PBEF/NAMPT/visfatin activates pro-inflammatory signalling in human vascular smooth muscle cells through nicotinamide phosphoribosyltransferase activity. *Diabetologia* **52**, 2455–2463.

Schilte, C., Couderc, T., Chretien, F., Sourisseau, M., Gangneux, N., Guivel-Benhassine, F., Kraxner, A., Tschopp, J., Higgs, S. & other authors (2010). Type I IFN controls chikungunya virus via its action on nonhematopoietic cells. *J Exp Med* **207**, 429–442.

Seymour, R. L., Rossi, S. L., Bergren, N. A., Plante, K. S. & Weaver, S. C. (2013). The role of innate versus adaptive immune responses in a mouse model of O'nyong-nyong virus infection. *Am J Trop Med Hyg* **88**, 1170–1179.

Sourisseau, M., Schilte, C., Casartelli, N., Trouillet, C., Guivel-Benhassine, F., Rudnicka, D., Sol-Foulon, N., Le Roux, K., Prevost, M. C. & other authors (2007). Characterization of reemerging chikungunya virus. *PLoS Pathog* **3**, e89.

Swiecki, M., Wang, Y., Gilfillan, S., Lenschow, D. J. & Colonna, M. (2012). Cutting edge: paradoxical roles of BST2/tetherin in promoting type I IFN response and viral infection. *J Immunol* **188**, 2488–2492.

Thio, C. L., Yusof, R., Abdul-Rahman, P. S. & Karsani, S. A. (2013). Differential proteome analysis of chikungunya virus infection on host cells. *PLoS ONE* **8**, e61444.

Tokarev, A., Suarez, M., Kwan, W., Fitzpatrick, K., Singh, R. & Guatelli, J. (2013). Stimulation of NF-κB activity by the HIV restriction factor BST2. *J Virol* **87**, 2046–2057.

Van den Bergh, R., Morin, S., Sass, H. J., Grzesiek, S., Vekemans, M., Florence, E., Tran, H. T., Imiru, R. G., Heyndrickx, L. & other authors (2012). Monocytes contribute to differential immune pressure on R5 versus X4 HIV through the adipocytokine visfatin/NAMPT. *PLoS ONE* **7**, e35074.

Veillette, M., Désormeaux, A., Medjahed, H., Gharsallah, N. E., Coutu, M., Baalwa, J., Guan, Y., Lewis, G., Ferrari, G. & other authors (2014). Interaction with cellular CD4 exposes HIV-1 envelope epitopes targeted by antibody-dependent cell-mediated cytotoxicity. *J Virol* **88**, 2633–2644.

Wang, P., Xu, T. Y., Guan, Y. F., Su, D. F., Fan, G. R. & Miao, C. Y. (2009). Perivascular adipose tissue-derived visfatin is a vascular smooth muscle cell growth factor: role of nicotinamide mononucleotide. *Cardiovasc Res* **81**, 370–380.

Wauquier, N., Becquart, P., Nkoghe, D., Padilla, C., Ndjoyi-Mbiguino, A. & Leroy, E. M. (2011). The acute phase of Chikungunya virus infection in humans is associated with strong innate immunity and T CD8 cell activation. *J Infect Dis* **204**, 115–123.

Werneke, S. W., Schilte, C., Rohatgi, A., Monte, K. J., Michault, A., Arenzana-Seisdedos, F., Vanlandingham, D. L., Higgs, S., Fontanet, A. & other authors (2011). ISG15 is critical in the control of Chikungunya virus infection independent of UbE1L mediated conjugation. *PLoS Pathog* **7**, e1002322.

Whitmire, J. K., Flavell, R. A., Grewal, I. S., Larsen, C. P., Pearson, T. C. & Ahmed, R. (1999). CD40–CD40 ligand costimulation is required for generating antiviral CD4 T cell responses but is dispensable for CD8 T cell responses. *J Immunol* **163**, 3194–3201.

Wikan, N., Sakoonwatanyoo, P., Ubol, S., Yoksan, S. & Smith, D. R. (2012). Chikungunya virus infection of cell lines: analysis of the East, Central and South African lineage. *PLoS ONE* **7**, e31102.